Journal of Colloid and Interface Science 326 (2008) 261–266

Contents lists available at ScienceDirect

Journal of Colloid and Interface Science

www.elsevier.com/locate/jcis

Characterization of crystal structure in binary mixtures of latex globules

Lei Liu, Shenghua Xu, Jie Liu, Zhiwei Sun *

Institute of Mechanics, Chinese Academy of Sciences, Beijing 100080, PR China

ARTICLE INFO

Article history:
Received 1 April 2008
Accepted 4 July 2008
Available online 16 July 2008

Keywords:
Colloidal crystal
Polystyrene
Kossel diffraction
Reflection spectra
The mean interparticle distance
Binary system

ABSTRACT

Colloidal crystals formed by two types of polystyrene particles of different sizes (94 and 141 nm) at various number ratios (94:141 nm) are studied. Experiments showed that the formation time of crystals lengthens as the number ratio of the two components approaches 1:1. The dependence of the mean interparticle distance (D_0), crystal structure and alloy structure on the number ratio of the two types of particles was studied by means of Kossel diffraction technique and reflection spectra. The results showed that as the number ratio decreased, the mean interparticle distance (D_0) became larger. And the colloidal crystal in binary mixtures is more preferably to form the bcc structure. This study found that binary systems form the substitutional solid solution (sss)-type alloy structure in all cases except when the number ratio of two types of particles is 5:1, which results instead in the superlattice structure.

1. Introduction

The colloidal crystal is a useful model for studying metals and protein crystals. Since the units in colloidal crystals are several orders of magnitude larger than those of atomic or molecular crystals, it is possible to observe and analyze colloidal crystals by much simpler optical methods. The mechanism of colloidal crystal growth has hitherto been studied by many researchers for the two groups of colloidal crystals: diluted and deionized aqueous suspension (soft crystal) [1–16] and concentrated suspension in refractive-index-matched organic solvents (hard crystal) [17–20]. Early studies focused on the colloidal crystals formed by monodispersed particles, meaning that both the material and the size of the particles in the colloidal crystals were the same. Significant attention has also been paid to the colloidal crystals in binary systems. When particles with two different sizes and surface charges are mixed together, the situation becomes more complicated than in single-component suspensions. For the single-component suspensions, crystal properties depend on the radius, the surface charge density and concentration of the particles, the salt concentration, as well as the temperature. For binary-component suspensions, there are two additional parameters, namely, the diameter ratio (to the charged sphere the diameter includes the Debye screening length) and fraction of each species. The resulting structures and properties can be manifold, as both the sizes and proportion of the two types of particles can be varied.

Among studies of the colloidal crystals in binary systems, most dealt with hard-sphere or hard-sphere–polymer mixtures of large size differences, where superlattice formation, phase separation and crystallization kinetics were observed [21–24]. For deionized aqueous suspensions, there exist only a few reports concerning their phase behavior [25–27] and other properties, for instance, rigidity and crystallization kinetics [28–31]. Studies concerning their crystal structures are even fewer. Among these efforts, Hachisu and Yoshimura studied alloy structures formed by binary systems consisting of two types of latex particles of different sizes (270 and 550 nm) [32,33] by metallurgical microscope. However, the results revealed only some local information. Shinohara observed the structure of colloidal crystals in mixed sedimenting dispersions of latex and silica particles (55.8 and 170 nm) by means of the Kossel diffraction method [34]. As the density of silica particles is 2.2 g/cm^3, gravity made the silica particles sedimentate quickly. Thus the number ratio of the two types of particles at different cuvette heights could be different. Furthermore, silica particles are segregated upward by the small latex particles. These factors made it difficult to study the influence of varying the number ratio on the colloidal crystal structure from Shinohara's results. To solve this problem, ideally, the experiments should be performed under microgravity conditions to avoid the effect of sedimentation or by using appropriate particles with a density matched medium to minimize the sedimentation effect.

Since the density of polystyrene particles is close to that of water, if particles are smaller, the sedimentation effect should not be significant. Therefore, we chose binary systems consisting of polystyrene (PS) particles of different sizes (diameters 94 and 141 nm). By analysis via UV–vis spectrophotometer, we found that the turbidities at different heights of the sample cell were approxi-

* Corresponding author. Present address: Institute of Mechanics, Chinese Academy of Sciences, Beijing 100080, PR China. Fax: +86 10 82544096.
E-mail address: sunzw@imech.ac.cn (Z. Sun).

0021-9797/$ – see front matter
doi:10.1016/j.jcis.2008.07.017

mately the same after three days. This result implies that the effect of gravity is not noticeable in our experiments. Therefore, the two types of PS particles can be blended symmetrically, which makes it possible to more accurately examine the influence of the number ratio on the crystal structure. Since microscopes cannot be used to observe such small particles, the Kossel diffraction method and reflection spectra were adopted in our experiment to study the dependence of formation time, interparticle distance (D_0), and alloy structures on the number ratio of two types of particles at the same volume fraction. We found in the binary systems that the crystal structure is dependent not only on volume fraction but also on the number ratio of two types of particles.

2. Materials and methods

2.1. Materials

The charged polystyrene colloidal particles used in the experiments were prepared by emulsion polymerization. The diameters of latex particles measured by an electron microscope were 94 and 141 nm, respectively. The surface charge density of latex particles of 9.1 and 10.0 μC/cm^2 respectively were determined by conductometric titration.

To increase the electric repulsion between particles, ions other than H^+ and OH^- in the solution were largely removed. The PS suspensions were ultra-filtrated with pure water repeatedly and treated by anion-and-cation exchange resins (G501-X8 (D), Bio-Rad Laboratories, USA). The water used for sample suspension was obtained from a Milli-Q water system.

In order to study the influence of the composition ratios of two types of latex particles on colloidal crystals, the samples of the different number ratios (the number density of 94:141 nm) at the volume fraction $\Phi = 0.015$, 0.020 and 0.025 are prepared. The samples form colloidal crystal by self-assembly method after introduced into regular rectangular quartzes cell with dimensions 1 mm × 10 mm × 45 mm. The Kossel diffraction method and reflection spectroscopy were used to characterize the colloidal crystals formed in different situations.

2.2. Kossel diffraction method

Diffraction phenomena were measured using an apparatus similar to that employed by Tsuyoshi Yoshiyama [4,35]. A fine laser beam directed through an incident aperture with a 1.0 mm^2 pinhole randomly interacts with a disordered region that exists between crystal grains in the suspension so that the region becomes a point light source of divergent beams. Parts of the divergent beams from the point light source within the crystal are reflected by lattice planes only at angles satisfying Bragg's law. The reflected beams from a set of planes with the index hkl will then generate the surface of a cone (Kossel cone) whose central axis is parallel to the reciprocal lattice vector G_{hkl}. The magnitude G_{hkl} of the reciprocal lattice vector and the semiapex angle α_{hkl} of the cone are related by:

$$G_{\mathrm{hkl}} = \frac{2n}{\lambda}\cos\alpha_{\mathrm{hkl}}, \tag{1}$$

where λ/n is the wavelength of the beam within the crystal and n is the refractive index of the crystal.

Coordinates of three points on a Kossel line are sufficient to define the geometry of the Kossel cone within the colloidal crystal. Therefore, by measuring the coordinates of three points on a Kossel line, we are able in principle to determine the semiapex angle α_{hkl} of the Kossel cone and the direction of its axis. Then the magnitude of the reciprocal lattice vector G_{hkl} is obtained from Eq. (1), since the wavelength λ of the beam in vacuum and the refractive index n of the crystal are known beforehand. For crystals with a cubic structure, the interplanar spacing d_{hkl}, which is the inverse of the magnitude G_{hkl} of the reciprocal lattice vector, is given by the lattice constant l_a as:

$$d_{\mathrm{hkl}} = \frac{1}{G_{\mathrm{hkl}}} = \frac{l_a}{\sqrt{h^2+k^2+l^2}}. \tag{2}$$

In this experiment, the specimens were examined by laser (He–Ne: $\lambda = 532$ nm) in a dark box at 25 °C temperature. The direction of the incident beam was vertical to the broad side of the rectangle sample cell.

2.3. Reflection spectroscopy

A fiber optic spectrometer (Avantes, Avaspec-2048, Netherlands) with a tungsten halogen light source (Avalight-HAL, Netherlands) and a bifurcated fiber optic cable was used to scan the light intensity reflected from the sample cell over a wavelength range. The relationship between the peak wavelength and the lattice spacing d is given by Bragg's equation,

$$m\lambda = 2d\sin\theta \tag{3}$$

where m is the diffraction order and θ is the diffraction angle. Bragg's equation is applied to the colloidal crystals with refraction relationships between air–glass and glass–sample interfaces. Considering the colloidal crystals for close-packed lattices, the relationship between particle distance $D_{\mathrm{Exp\ (rs)}}$ and wavelength λ is given by

$$m^2\lambda^2 = (8/3)D^2_{\mathrm{Exp\ (rs)}}\left(n_s^2 - n_g^2\cos^2\theta\right). \tag{4}$$

In this experiment, setting $m = 1$ or 2, $\theta = 90°$, $n_s = 1.333$ and $n_g = 1.0003$, the following equation holds:

$$D_{\mathrm{Exp\ (rs)}} = 0.459 \text{ m}. \tag{5}$$

3. Results

3.1. Dependence of the formation of crystals on the composition ratios of two types of latex particles

In our experiment, the formation time of samples of the binary systems with different number density ratios were studied at the volume fractions $\Phi = 0.015$, 0.020 and 0.025, respectively. Our results showed that when the volume fraction was kept the same, the formation time could be quite different for different number ratios. Taking $\Phi = 0.02$ as an example, the samples with number ratios 1:0, 5:1, 1:5 and 0:1 displayed iridescence before their introduction into the cuvettes, implying that crystallization already occurred, while for the mixtures of 2:1, 1:1 and 1:2 no crystallization was observed within such a short period of time. As soon as they were introduced into the cuvettes, the mixtures of 1:0 and 0:1 immediately began to display iridescence throughout the container. The mixtures of 5:1 and 1:5 began to display iridescence within a few minutes after their introduction into the cuvettes. For the mixtures of 2:1, 1:1 and 1:2, crystallization appeared until the third day, the tenth day, and half a day, respectively, after their introduction into the cuvettes. At $\Phi = 0.015$, 0.020 and 0.025 the formation times of the samples are shown in Table 1. From Table 1, we can see that the formation times of crystals increases as the number ratio approaches 1:1. This result demonstrates an obvious dependence of the colloidal crystal formation time on the polydispersity indices, which include the size polydispersity index (SPD) and the charge polydispersity index (CPD).

The SPD and CPD are quantified in terms of the standard deviation of the size and charge with respect to their mean respectively.

$$\mathrm{SPD} = \left(\langle d^2\rangle - \langle d\rangle^2\right)^{1/2}/\langle d\rangle,$$

Table 1
The formation time of the mixture of the various number ratio at $\Phi = 0.02$

	1:0	5:1	2:1	1:1	1:2	1:5	0:1
0.015	A few seconds	A few minutes	2 days	9 days	A few minutes	A few seconds	A few seconds
0.020	A few seconds	A few minutes	3 days	10 days	Half a day	A few minutes	A few seconds
0.025	A few seconds	4 h	4 days	11 days	Half an hour	A few seconds	A few seconds

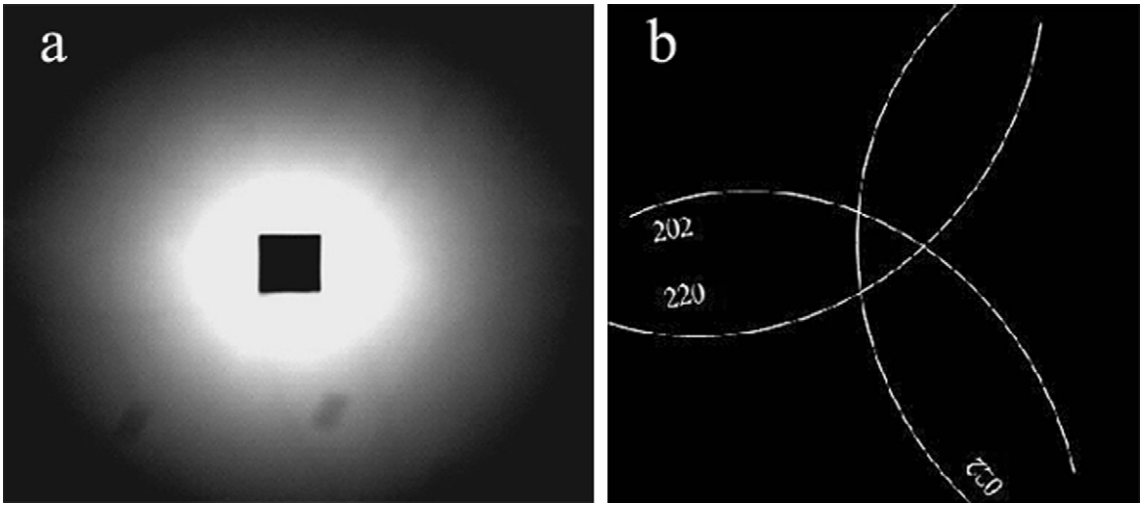

Fig. 1. (a) The image of Kossel pattern of the mixture of the number ratio 5:1 at $\Phi = 0.02$. (b) The sketch map of Fig. 1a. The threefold symmetry of the pattern shows that the colloidal crystal has the normal FCC structure. Indices of Kossel lines are shown in Fig. 1b.

and

$$\mathrm{CPD} = \left(\langle Z^2\rangle - \langle Z\rangle^2\right)^{1/2}/\langle Z\rangle,$$

where $\langle d\rangle$ and $\langle Z\rangle$ are the average diameter and average charge number respectively.

The charge polydispersity index was determined by the surface charge density of the particles and the size of the particles. Since the interparticle distance is several times larger than the particles' diameters in the colloidal crystal, the charge polydispersity index plays a more important role than the size polydispersity index [36]. Considering that the charge polydispersity indices increased as the number ratio approached 1:1, our experiments showed that the formation of colloidal crystals became more difficult as the charge polydispersity indices increased.

However, the crystallization times of the number ratio 1:2 and 1:5 are, respectively, longer than those of the number ratio 2:1 and 5:1. A probable explanation for the results is that longer diffusion times are required for the site exchanges of different sized or charged particles for accomplishing their crystallization. At the same volume fraction, the total number densities of the number ratio 1:2 and 1:5 are, respectively, more than those of the number ratio 2:1 and 5:1. So the longer diffusion times are required for the number ratio 1:2 and 1:5.

3.2. Dependence of crystal structure on the composition ratios of two types of latex particles

The crystal structure and the mean interparticle distances of the binary systems with different number density ratios at the volume fractions $\Phi = 0.015$, 0.020 and 0.025, respectively, were determined through analysis of the Kossel line diffraction image of the samples. At $\Phi = 0.02$ the colloidal crystals of the different number ratios, 1:0 and 5:1 showed FCC structures, while those of 2:1, 1:1, 1:2 and 1:5 had BCC structures. As typical examples, the Kossel line diffraction images of $\Phi = 0.02$, 5:1 and 1:5 mixtures are shown in Figs. 1 and 2, respectively. The threefold symmetry of the pattern in Fig. 1 shows that the colloidal crystal has a normal FCC structure, while the twofold symmetry of the pattern in Fig. 2 shows that the colloidal crystal has a BCC structure. However, from the Kossel pattern of the 0:1 mixture, we discovered the coexistence of the FCC structure and the BCC structure in the same crystal grain. In order to study the dependence of crystal structure on the composition ratios of two types of latex particles, we analyzed the crystal structures of samples of the different number density ratios at the volume fraction $\Phi = 0.015$ and 0.025. We found the crystal structures of the different number density ratios at $\Phi = 0.015$ and 0.025 are the same as that of $\Phi = 0.020$ except that of the 0:1 mixture. At $\Phi = 0.015$ the crystal structure of the 0:1 mixture is BCC. At $\Phi = 0.025$ the crystal structure of the 0:1 mixture is FCC. This result is consistent with the fact that the colloidal crystal in monodispersed system will tend to form FCC structure for large volume fraction. The crystal structures of the all samples are shown in Table 2. From Table 2 the colloidal crystal in binary mixtures is easy to form the BCC structure.

We assume that this result is correlated to the formation process of colloidal crystals in binary mixtures. As mentioned in the last section, the different sized or charged particles have to properly exchange their positions in order to form colloidal crystals in binary mixtures. Therefore, some particles that did not fit their crystal sites would not be able to join the formation of colloidal crystal. This may result in a reduction of volume fraction in which the particles form colloidal crystals. As the volume fraction decreased, the colloidal crystal has the tendency to form BCC structure [7], as shown in Table 2.

3.3. Dependence of the mean interparticle distance on the composition ratios of two types of latex particles

The mean interparticle distance is an important feature of the colloidal crystal. We studied the influence of the number ratio of two types of particles on the mean interparticle distance by analysis of Kossel diffraction and reflection spectra. As mentioned above, for the Kossel line diffraction method, the lattice con-

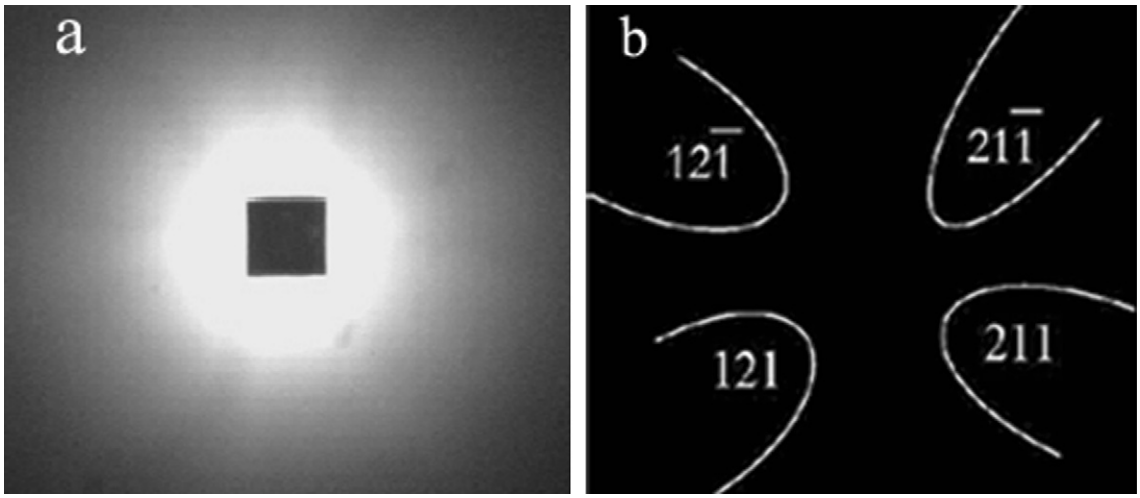

Fig. 2. (a) The image of Kossel pattern of the mixture of the number ratio 1:5 at $\Phi = 0.02$. (b) The sketch map of Fig. 2a. The twofold symmetry of the pattern shows that the colloidal crystal has the BCC structure. Indices of Kossel lines are shown in Fig. 2b.

Table 2
The crystal structure of the mixture of the various number ratio at $\Phi = 0.015, 0.02$ and 0.025

	1:0	5:1	2:1	1:1	1:2	1:5	0:1
0.015	fcc	fcc	bcc	bcc	bcc	bcc	bcc
0.020	fcc	fcc	bcc	bcc	bcc	bcc	fcc and bcc
0.025	fcc	fcc	bcc	bcc	bcc	bcc	fcc

stant (l_a) and the interplanar spacing (d_{hkl}) can be obtained from Eqs. (1) and (2). The relationship of the mean interparticle distance ($D_{\mathrm{Exp\ (kl)}}$) and the lattice constant (l_a) or the interplanar spacing (d_{hkl}) can be approximated as [2]:

$$\text{for FCC:} \quad D_{\mathrm{Exp\ (kl)}}/0.707 = 3^{1/2} d_{\mathrm{hkl}} = l_a, \tag{6}$$

$$\text{for BCC:} \quad D_{\mathrm{Exp\ (kl)}}/0.866 = 3^{1/2} d_{\mathrm{hkl}} = l_a. \tag{7}$$

For the reflection spectra method, the mean interparticle distance can be obtained from Eq. (4).

The mean interparticle distances evaluated by analysis of the Kossel line and the reflection spectroscopy are summarized in Table 3. From Table 3 we can see that the mean interparticle distances increase as the number ratio of the two types of particles decrease.

As have known, the crystal properties depend on the radius, the surface charge density and the concentration of the particles, the salt concentration, and the temperature. In our experiment, the ions other than H^+ and OH^- in the solution had been removed to the extent that the salt effect in the suspension could be neglected. The total concentration of the two types of particles and the temperature were kept constant in the experiments. Therefore, the mean interparticle distance was determined by the radius and the surface charge density of the particles.

The mean interparticle distance can be embodied by the effective diameter of particles. The effective diameter of particles (including the Debye screening length) is given by the diameter plus twice the Debye screening length [37]. When the effective diameter is shorter than the observed interparticle distance, a gas-like distribution forms. When the effective diameter is close to or slightly shorter than the observed interparticle distance, a liquid-like distribution occurs. When the effective diameter is comparable to or larger than the observed interparticle distance, the distribution of sphere is a crystal ordering [37]. The Debye screening length, D_l, is given by the equation

$$D_l = \left(4\pi e^2 n/\varepsilon k_B T\right)^{-1/2}, \tag{8}$$

where e is the electronic charge, ε is the dielectric constant of the solvent, and n is the concentration of diffusible or free-state cations and anions in suspension. Thus, n is the sum of the concentrations of diffusible counterions (n_c), foreign salt (n_s) and both H^+ and OH^- from the dissociation of water (n_0).

$$n = n_c + n_s + n_0 = \left(2 \times 10^{-7} + (Q_A \beta_A \Phi_A/1.606 d_A) + (Q_B \beta_B \Phi_B/1.606 d_B)\right) \times N_A \times 10^{-3}, \tag{9}$$

where A and B are the different particles, respectively, Q_A and Q_B are the surface charge density of particles A and B, respectively, Φ is the volume fraction, and β is the fraction of free-state counterions. In our case, β_A and β_B were assumed to be 0.1. The Debye screening length D_l from Eqs. (8) and (9) becomes larger when increasing the number of particles of the larger size. The result is consistent with the experimentally evaluated Debye screening length, $D_l = (D_{\mathrm{Exp\ (rs)}} - (d_a + d_b)/2)/2$, listed in Table 3. Thus, the mean interparticle distance became larger as the number ratio decreased.

3.4. Dependence of alloy structure on the composition ratios of two types of latex particles

We also studied colloidal crystal alloy structures and the mean interparticle distance of the samples by reflection spectroscopy. Fig. 3 shows the reflection spectra of the samples at $\Phi = 0.02$. In Fig. 3 the colloidal crystals of different number ratios, 1:0 and 2:1, have one reflection peak, respectively. Because the mixtures of 1:0 and 2:1 have the FCC and BCC structures respectively, the reflection peaks of the mixtures of 1:0 and 2:1 were assigned to the primary peak of 111 and 110 planes. In the mixtures of 1:1, 1:2 and 1:5 two reflection peaks appeared. As the mixtures of 1:1, 1:2 and 1:5 have the BCC structures, the peaks show the primary and secondary Bragg's reflections peak of 110 planes.

Generally speaking, if the wavelengths of two peaks were always close together, with a difference of only 1.025 in the ratios of their wavelengths, the longer wavelength is associated with the face-centered cubic lattice and the shorter wavelength corresponds to the body-centered cubic lattice [28]. Hence, three reflection peaks for the spectrum of the mixtures of 0:1 at 459.39, 878.89 and 909.07 nm are related to the primary peak of the face-centered cubic (fcc), body-centered cubic (bcc) and the secondary peak of the face-centered cubic (fcc) lattices, respectively. Surprisingly, we found that several little peaks, except for the primary peak of the face-centered cubic appeared for the mixtures of 5:1.

Table 3
The mean interparticle distance of the mixture of the various number ratio at $\Phi = 0.02$

	1:0	5:1	2:1	1:1	1:2	1:5	0:1
D_{Calc}	313.45	339.56	368.18	393.12	415.25	435.70	466.84
λ							
$m = 2$				425.73	434.43	429.98	475.48
$m = 1$	552.90	624.37	690.81	836.12	855.08	852.41	937.24
$D_{Exp\ (rs)}$							
$m = 2$				390.82	398.81	394.72	436.49
$m = 1$	253.78	286.59	316.71	383.78	392.48	391.26	430.19
$D_{Exp\ (kl)}$	263.71	300.47	330.05	385.75	388.88	390.77	419.07
D_l	79.50	86.05	99.61	134.90	139.07	137.75	157.92
γ	–	0.85	0.86	0.89	0.89	0.89	–

rs: reflection spectra; kl: Kossel diffraction; D_{Calc}: the calculated mean interparticle distance from Eqs. (10), (11) and (12); $D_{Exp\ (rs)}$: the experimentally evaluated mean interparticle distance by reflection spectroscopy analysis; $D_{Exp\ (kl)}$: the experimentally evaluated mean interparticle distance by Kossel line analysis; λ: the wavelength from the reflection spectroscopy; m is the diffraction order; D_l: the experimentally evaluated Debye screening length; γ: the effective size ratio of two types of particles (ps94/ps140).

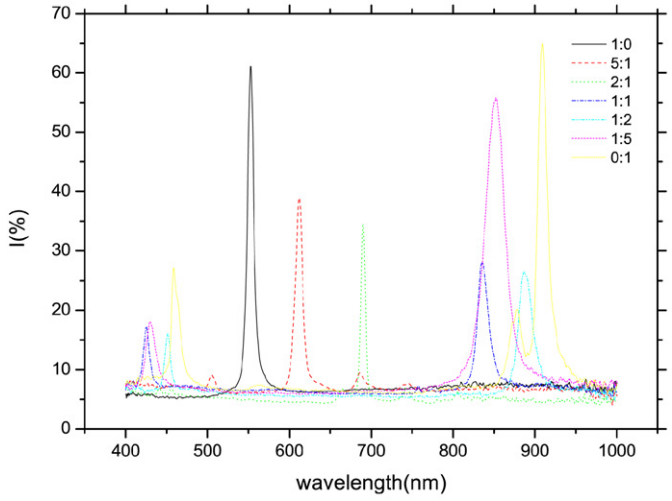

Fig. 3. The reflection spectra of the mixture of the various number ratio at $\Phi = 0.02$.

According to the above criterion, the several little peaks were neither the secondary peaks of the face-centered cubic (fcc) lattices nor the peak of the body-centered cubic. From Ref. [28] it can be concluded that the superlattice structures occurred.

In order to confirm the alloy structure of the samples, we compared the calculated mean interparticle distances (D_{Calc}) to their experimental values (including Kossel diffraction $D_{Exp\ (kl)}$ and reflection spectra $D_{Exp\ (rs)}$). The mean interparticle distance, when two different types of particles were distributed in the substitutional solid solution (sss) or body-centered cubic (bcc), is calculated using Eq. (10) [29]

$$D_{Calc} = \left[\left(\Phi_1/0.68d_1^3\right) + \left(\Phi_2/0.68d_2^3\right)\right]^{-1/3}, \quad (10)$$

where Φ_1 and Φ_2 are the volume fractions of particles 1 and 2, respectively, and d_1 and d_2 are the diameters of each particle.

When the monodispersed particles had a face-centered cubic (fcc) distribution, the calculated values of the mean interparticle distance (D_{Calc}) were obtained as [7]:

$$D_{Calc} = 0.905d\Phi^{-1/3}. \quad (11)$$

When the monodispersed particles had a body-centered cubic (bcc) distribution, the calculated values of the mean interparticle distance (D_{Calc}) was obtained as [7]:

$$D_{Calc} = 0.875d\Phi^{-1/3}, \quad (12)$$

where Φ are the volume fractions of particles and d are the diameters of the sphere.

The calculated mean interparticle distance (D_{Calc}) from Eqs. (10), (11) and (12) are listed in Table 3. From Table 3 we found the calculated values are larger than the experimentally evaluated values. This is due to the existence of the long range weak attraction in addition to the short range strong repulsion among colloidal particles [7]. The ratio (γ) of the effective diameters of two types of particles is the crucial factor in determining alloy structure. Binary mixtures of hard-sphere colloidal particles with the ratio of the effective sizes [37] (including no the Debye screening length) of two types of particles $\gamma = 0.58$ were observed to form AB_2 and AB_{13} superlattice structures [21]. For soft-sphere colloidal particles, when the ratio of the effective sizes (including the Debye screening length) of two types of particles $\gamma = 0.77 - 0.84$ and $\gamma > 0.85$, $MgCu_2$-type superlattice structure and substitutional solid solution alloy structure are formed, respectively [28]. From Table 3 we found that the ratios (γ) of the effective sizes of two types of particles including the Debye screening length were larger than 0.85, except when the number ratio of two particles was 5:1. Thus, our experimental result was consistent with the conditions of forming the superlattice structure and the substitutional solid solution alloy structure.

4. Summary

We observed binary systems consisting of two types of latex particles of different sizes (94 and 141 nm). When the two dispersions were mixed together with different number ratios, they can form crystal structures. However, when the number ratio of the two parts approaches 1:1, the formation time of crystals lengthens. This result shows an obvious dependence of the colloidal crystal formation time on polydispersity indices.

Based on analysis of the Kossel diffraction and the reflection spectra, our experiments showed that:

(a) The colloidal crystal in binary mixtures is more preferably to form the BCC structure. This is because some particles may not be in a proper position to join the crystal structures, making the actual volume fraction to form the crystals smaller.

(b) The mean interparticle distance becomes larger as number ratio (94:141 nm) decreased. This supports the assumption that the mean interparticle distance is more likely to take the Debye screening length.

(c) The binary systems in this study generally form the sss-type alloy structure except forming the superlattice structure for the case that the number ratio of two types of the particles is 5:1. The calculated ratios of the effective diameters (γ) of two types of particles show that our experimental result was consistent with the conditions for forming the superlattice structure and the substitutional solid solution alloy structure.

Acknowledgments

This work is supported by Grant Nos. 20473108, 10672173 and 10432060 from the National Natural Science Foundation of China and the "Chuang-xin Project" of the Chinese Academy of Sciences (including 0518181162).

References

[1] B.J. Ackerson, N.A. Clark, Phys. Rev. Lett. 46 (1981) 123.
[2] T. Okubo, A. Tsuchida, Forma 17 (2002) 141.
[3] D.J.W. Aastuen, N.A. Clark, Phase Transition 21 (1990) 139.
[4] T. Yoshiyama, Polymer 27 (1986) 827.
[5] N.A. Clark, A. Hurd, B.J. Ackerson, Nature 281 (1979) 57.
[6] T. Okubo, J. Chem. Phys. 93 (1990) 8276.
[7] T. Yoshiyama, I. Sogami, N. Ise, Phys. Rev. Lett. 53 (1984) 2153.
[8] P. Wette, H.J. Schope, T. Palberg, J. Chem. Phys. 123 (2005) 174902.
[9] A. Tsuchida, E. Takyo, Colloid Polym. Sci. 282 (2004) 1105.
[10] T. Shinohara, T. Yoshiyama, Langmuir 17 (2001) 8010.
[11] S. Hachisu, S. Yoshimura, Nature 283 (1980) 188.
[12] K. Yoshinaga, K. Fujiwara, Langmuir 21 (2005) 4471.
[13] T. Shinohara, T. Yoshiyama, Phys. Rev. E 70 (2004) 062401.
[14] T. Okubo, J. Colloid Interface Sci. 228 (2000) 151.
[15] R.S. Crandall, R. Williams, Science 198 (1977) 293.
[16] K. Furusawa, N. Tomotsu, J. Colloid Interface Sci. 93 (1983) 504.
[17] W.B. Russel, J. Zhu, M. Li, R. Rogers, W.V. Meyer, R.H. Ottewill, Crew Space Shuttle Columbia, W.B. Russel, P.M. Chaikin, Nature 387 (1997) 883.
[18] D.A. Weitz, Science 303 (2004) 968.
[19] A.R. Bausch, M.J. Bowick, A. Cacciuto, A.D. Dinsmore, M.F. Hsu, D.R. Nelson, M.G. Nikolaides, A. Travesset, D.A. Weitz, Science 299 (2003) 1716.
[20] M.G. Nikolaides, A.R. Bausch, M.F. Hsu, A.D. Dinsmore, M.P. Brenner, C. Gay, D.A. Weitz, Nature 420 (2002) 299.
[21] P. Bartlett, R.H. Ottwill, P.N. Pusey, Phys. Rev. Lett. 68 (1992) 3801.
[22] P. Bartlett, R.H. Ottwill, P.N. Pusey, J. Chem. Phys. 93 (1990) 1299.
[23] S.I. Henderson, W. van Megen, Phys. Rev. Lett. 80 (1998) 879.
[24] A.B. Schofield, P.N. Pusey, P. Radcliffe, Phys. Rev. E 72 (2005) 031407.
[25] P.D. Kaplan, J.L. Rouke, A.G. Yodh, D.J. Pine, Phys. Rev. Lett. 72 (1994) 582.
[26] A. Meller, J. Stavans, Phys. Rev. Lett. 68 (1992) 3645.
[27] T. Okubo, H. Fujita, Colloid Polym. Sci. 274 (1996) 368.
[28] T. Okubo, H. Ishiki, Colloid Polym. Sci. 279 (2001) 571.
[29] T. Okubo, H. Ishiki, Colloid Polym. Sci. 278 (2000) 202.
[30] P. Wette, H.J. Schope, J. Liu, J. Chem. Phys. 122 (2005) 144901.
[31] J. Liu, T. Palberg, Prog. Colloid Polym. Sci. 123 (2004) 222.
[32] S. Hachisu, S. Yoshimura, Nature 283 (1980) 188.
[33] S. Hachisu, S. Yoshimura, Prog. Colloid Polym. Sci. 68 (1983) 59.
[34] T. Shinohara, T. Kurokawa, T. Yoshiyama, Phys. Rev. E 70 (2004) 062401.
[35] L. Liu, S.H. Xu, J. Liu, Acta Phys. Sinica 55 (2006) 6168.
[36] B.V.R. Tata, Curr. Sci. 80 (2001) 984.
[37] T. Okubo, Acc. Chem. Res. 21 (1988) 281.